Thermoresponsive Polymer Micropatterns Fabricated by Dip-Pen Nanolithography for a Highly Controllable Substrate with Potential Cellular Applications

By Stacey Laing,#[†] Raffaella Suriano,#[‡] Dimitrios A. Lamprou,[§] Carol-Anne Smith,[∥] Matthew J. Dalby,[∥] Samuel Mabbott,[†] Karen Faulds[†] and Duncan Graham[†]*

 # both authors contributed equally to this work

† Centre of Molecular Nanometrology, Technology and Innovation Centre, University of Strathclyde, 99 George Street, Glasgow G1 1RD, United Kingdom.

‡ Department of Chemistry, Materials and Chemical Engineering "Giulio Natta", Politecnico di Milano, Piazza Leonardo da Vinci 32, 20133 Milano, Italy.

§ Strathclyde Institute of Pharmacy and Biomedical Sciences (SIPBS), University of Strathclyde, 161 Cathedral Street, Glasgow G4 0RE, United Kingdom. EPSRC Centre for Innovative Manufacturing in Continuous Manufacturing and Crystallisation (CMAC), University of Strathclyde, Technology and Innovation Centre, 99 George Street, Glasgow G1 1RD, United Kingdom.

‖ Centre for Cell Engineering, Institute for Molecular, Cell and Systems Biology, University of Glasgow, Glasgow G12 8LT, United Kingdom.

KEYWORDS

thermoresponsive polymers, smart hydrogel structures, polymer arrays, dip-pen nanolithography, atomic force microscopy.

ABSTRACT

We report a novel approach for patterning thermoresponsive hydrogels based on N,N-diethylacrylamide (DEAAm) and bifunctional Jeffamine ED-600 by dip-pen nanolithography (DPN). The direct writing of micron-sized thermoresponsive polymer spots was achieved with efficient control over feature size. A Jeffamine-based ink prepared through the combination of organic polymers, such as DEAAm, in an inorganic silica network was used to print thermosensitive arrays on a thiol-silanised silicon oxide substrate. The use of a Jeffamine hydrogel, acting as a carrier matrix, allowed a reduction in the evaporation of ink molecules with high volatility, such as DEAAm, and facilitated the transfer of ink from tip to substrate. The thermoresponsive behaviour of polymer arrays which swell/de-swell in aqueous solution in response to a change in temperature was successfully characterised by atomic force microscopy (AFM) and Raman spectroscopy: a thermally-induced change in height and hydration state was observed, respectively. Finally, we demonstrate that cells can adhere to and interact with these dynamic features and exhibit a change in behaviour when cultured on the substrates above and below the transition temperature of the Jeffamine/DEAAm thermoresponsive hydrogels. This

demonstrates the potential of these micropatterned hydrogels to act as a controllable surface for cell growth.

INTRODUCTION

Hydrogels are three-dimensional polymer networks which exhibit a high level of biocompatibility due to their ability to trap water and biological fluids.[1,2] Some hydrogels undergo changes in swelling or network structure in response to external stimuli such as pH,[3] temperature,[4,5] light,[6,7] ionic strength[3] and electric field.[8] The development of such materials has recently received considerable interest due to the potential applications in a vast range of areas.[9,10] Of the possible stimuli, temperature is the most widely studied due to the prospective use of thermoresponsive polymers in biological systems, as well as the relatively simple control of temperature as an external stimulus.[11,12]

Thermoresponsive polymers in aqueous solution undergo a phase transition at a certain temperature, which causes a change in the solubility of linear polymer chains in water. At this phase transition temperature, a given polymer–water mixture passes from a one-phase system to a two-phase system or vice versa. Polymers which become soluble upon heating have an upper critical solution temperature (UCST), while systems whose solubility in water increases upon cooling have a lower critical solution temperature (LCST).[13] The majority of thermoresponsive systems reported in the literature exhibit a LCST in aqueous solution, such as poly(N-isopropylacrylamide), polysaccharides, and block copolymers of poly(ethyleneoxide) (PEO) and poly(propyleneoxide) (PPO).[14] The LCST-type transition takes place as a result of a local structural transition which involves water molecules surrounding macromolecular chains in

solution: water-polymer interactions are thermodynamically favoured below the LCST and by increasing the temperature above the LCST, the hydrophobic backbone and non-polar groups of the polymer tend to interact and aggregate. Such changes in the hydration state of the polymer chains are attributed both to the breakdown of polymer-water hydrogen bonding interactions, and to the "hydrophobic effect" which causes a local ordered structure like a hydrated shell between the molecules of water surrounding the hydrophobic groups of the polymer.[15,16] At the molecular level, this phase transition also leads to a volume transition from a coiled state of the polymer to the collapsed or globular state, in which hydrophobic interactions can occur between the polymer molecules. Accordingly, polymer chains which are completely soluble in water at temperatures below the LCST undergo a precipitation in aqueous solutions as the temperature is increased beyond the LCST. In the case of crosslinked hydrogels, in water at temperatures below the LCST, they cannot be dissolved due to the covalent bonds between polymer chains but they will be hydrophilic and therefore "swollen"; whereas when the temperature goes above the LCST, the hydrogel becomes hydrophobic and will thus "de-swell". By comparison with the corresponding linear polymer molecules, the temperature sensitivity of these gels similarly occurs due to a delicate balance of specific interactions between the water molecules and the monomer units and results in changes of enthalpy and entropy of mixing according to the Flory-Huggins theory.[17] These controlled conformational and thermodynamic changes can be exploited for their potential use in a variety of applications such as cell culture,[18-22] thermally controlled drug delivery,[23-25] protein separation,[26-28] microactuators[29-31] and microfluidic devices.[32,33] Many of these applications involve the formation of a switchable substrate, either by coating the entire surface with a layer of thermoresponsive polymer, or by producing polymer patterns which allow spatially controlled thermoresponsive features.

Previous patterns of thermoresponsive polymers on a surface involve the formation of polymer films or polymer brushes created by, for example, electron beam lithography,[34] microcontact printing[35] or nanografting.[36] These approaches involve patterning of an initiator followed by atom transfer radical polymerisation (ATRP) for the production of polymers. However, direct printing of polymer patterns onto a surface allows further control of feature size and shape and can provide a switchable substrate with highly tuneable topography.[37]

Dip-pen nanolithography (DPN) is a direct-write technique which uses an atomic force microscope (AFM) tip to "write" molecular "inks" onto a surface with extremely high accuracy and resolution.[38] The patterning of polymers and hydrogels by DPN has been an area of significant interest over recent years and many useful applications have been investigated.[39-42] Lee *et. al.* used thermal dip-pen nanolithography (tDPN) to produce nanostructures of a thermoresponsive polymer, poly(N-isopropylacrylamide) (PNIPAAm), for protein adsorption.[37] They printed lines of PNIPAAm and used adhesion force measurements to characterise the thermoresponse. Whilst they observed the expected hydrophilic-hydrophobic transition, they observed no change in topography which could potentially limit the use of their substrates for certain applications.

The work presented in this paper demonstrates the patterning of thermoresponsive polymers using DPN with significant control over feature size and shape. AFM and Raman spectroscopy have been utilised for the morphological and chemical characterisation of the printed arrays and to confirm the thermoresponsive behaviour of the micron-sized features when attached to the thiol-silanised silicon oxide surfaces. To demonstrate the potential use of these patterned substrates in biological applications, cells were cultured on the surfaces in order to investigate if

they would respond to the polymer features. The cells adhered to and interacted with the polymer microspots and a change in behaviour was observed across the transition temperature.

EXPERIMENTAL SECTION

Reagents and Materials

Acetone (≥99.5%), ethanol (≥99.8%), isopropyl alcohol (≥99.7%), glacial acetic acid (≥99.7%), 3-glycidoxypropyltrimethoxysilane (GPTMS) (≥98%), O,O‘-Bis(2-aminopropyl) polypropylene glycol-block-polyethylene glycol-block-polypropylene glycol (Jeffamine ED-600), poly(ethylene glycol) dimethacrylate, average M_n=550 (PEGDMA), 1-hydroxycyclohexyl phenyl ketone (photoinitiator) (99%), 3-(trimethoxysilyl)propyl methacrylate (TMSPM) (98%) and (3-mercaptopropyl)trimethoxysilane (MPTMS) (95%) were purchased from Sigma-Aldrich (Dorset, UK. N,N-diethylacrylamide (DEAAm) (>98%) was purchased from Tokyo Chemical Industry UK Ltd (Oxford, UK). All the chemicals were used as received except Jeffamine ED-600 which was dried under dynamic vacuum for 2 h before use to remove humidity. Silicon dioxide substrates with addressable registration marks to easily identify locations, 1D M-type pen arrays with 12 tips and a pitch of 66 μm, and multi-channel inkwell arrays were provided by Nanoink Inc. (Skokie, IL, USA).

Fabrication of thermoresponsive polymer arrays

Silicon dioxide substrates were cleaned by sonication in acetone, isopropanol and water, for 10 min in each solvent, and blown dry with nitrogen after each sonication bath. Substrates were then plasma-cleaned for 40 s at 50 % power, 72 cm^3 / min in oxygen. To silanise surfaces with MPTMS, the cleaned substrates were placed in an Erlenmeyer flask with 2 mL of MPTMS in a

nitrogen atmosphere for 30 minutes and then placed in an oven at 100 °C overnight before printing. For treating substrates with TMSPM,[43] 50 μL of TMSPM was diluted in 10 mL of ethanol and then 0.3 mL of dilute acetic acid (1:10 glacial acetic acid:water) was added just before use. This silane solution was poured onto the surfaces and allowed to react for 3 min. The excess was poured off and then substrates were rinsed with ethanol to remove the residual reagent and also dried under a nitrogen flux.

DPN experiments were performed using a Nanoink NLP 2000 nanolithography instrument. 1D M-type pen arrays were plasma cleaned for 40 s at 50% power (72 cm3 / minute) prior to use to remove any organic contamination. All the printing experiments were performed at 22-23 °C and in a relative humidity range of 25-35 %. DEAAm ink was prepared by mixing 500 mg of DEAAm, 0.5% wt of PEGDMA w.r.t. DEAAm (2.51 mg) and 3 % wt of photoinitiator w.r.t. DEAAm (15.46 mg) in a closed vial protected from light to minimise the activation of photoinitiator before printing. 0.3 μL of this mixture was then added to each inkwell and the tips were dipped in a 12-channel microfluidic inkwell. Once printed arrays were created, the substrates were exposed to a UV lamp for 10 min. For Jeffamine ink, stoichiometric amounts (2:1) of GPTMS (442.4 mg) and Jeffamine ED-600 (494.2 mg) were mixed in a closed glass vial under magnetic stirring for at least 2 h. 100 μL of distilled water was then added to the mixture and left under stirring for 10 more minutes. The printed Jeffamine arrays were left in a closed box overnight and then cured at 40°C for 1 h. The Jeffamine/DEAAm ink (mixed system) was made up by mixing the Jeffamine ink, prepared as described above, and the DEAAm ink, including also 1 % wt (5.05 mg) of TMSPM w.r.t. DEAAm, in a 1:1 ratio and then directly used for printing. These arrays were UV-cured for 10 min, left in a closed box overnight and eventually cured at 40 °C for 1 h.

Characterisation and instrumentation

The swelling behaviour of bulk thermoresponsive materials was analysed in duplicate at temperatures ranging from room temperature (20 °C) to 40 °C. Cured polymer samples were firstly placed in a lidded Petri dish filled with distilled water to swell at ambient temperature. After swelling for 72 h to reach equilibrium swelling, the hydrogels were blotted free of excess water with paper filter and their weights were measured using a scale. The samples were then moved in a beaker full of distilled water at 40 °C for 72 h. The weights at 40 °C were measured as previously described and the swelling ratio was calculated according the following formula:

$$\text{Swelling ratio (SR)} = W_{20°C} / W_{40°C}$$

where $W_{20°C}$ is the weight of the swollen samples at 20 °C and $W_{40°C}$ at 40 °C. The above process was repeated for a second time in order to verify the reversibility of swelling/shrinking characteristics.

AFM topography analysis in air was carried out on a DPN 5000TM nanofabrication system (Nanoink Inc., Skokie, IL, USA), in close-contact mode using ACT probes purchased from AppNano (nominal value of spring constant = 40 N/m).

The printed spots were analysed by a Witec Alpha300 R microscope (Ulm, Germany) provided with a 633 nm laser and a 100x objective. The grating was 600 g mm^{-1} and coupled to a thermoelectrically cooled charge-coupled device (CCD). Spectra were collected using 5 x 10 s accumulations.

AFM images in liquid were obtained by scanning the surface using a PeakForce QNM Scanning Probe Microscope (Digital Instruments, Santa Barbara, CA, USA). The AFM measurements were obtained using ScanAsyst-Fluid probes with a spring constant of 0.67 N/m (nominal value of tip radius = 2 nm).

Cell Culture

LE2 cells (a line of mouse lung capillary endothelia from B10D2 congenic mice, cd 133+)[44] were cultured in Hams F10 media (Sigma Aldrich, UK) supplemented with 3% FBS (Sigma Aldrich, UK), 2% antibiotic mix (60% v/v 200 mM L-glutamine (Sigma Aldrich, UK), 35% v/v penicillin/streptomycin (Sigma Aldrich, UK), 5% v/v fungizone (Invitrogen, UK)), 5 mL of 7.5% sodium bicarbonate (Sigma Aldrich, UK) and 10 mL ITS (100x, Life Technologies). Hams was chosen as it is CO_2 independent and thus can be simply cultured in different temperature environments.

Immunocytochemistry

After 4 days of culture, cells were fixed (10 mL 37% formaldehyde, 2 g sucrose in 90 mL PBS solution) for 15 minutes. Permeabilising buffer (10.3 g sucrose, 0.292 g NaCl, 0.06 g $MgCl_2$, 0.476 g HEPES, 0.5 mL Triton X, in 100 mL of H2O, at pH 7.2) was then added for 5 mins at 4°C. To block non-specific binding, samples were next incubated in 1% BSA/PBS for 5 mins at 37°C. H-vin 1 primary antibody (1:200, monoclonal antihuman raised in mouse (IgG1) Sigma Aldrich UK, in 1% BSA/PBS) was added for 1 hour along with rhodamine-conjugated phalloidin (1:100, Sigma Aldrich UK). Substrates were then washed three times in 0.5% Tween 20/PBS (5 minutes each). Secondary, biotin-conjugated antibody (1:50 in 1% BSA/PBS, antimouse (IgG) raised in horse, Vector laboratories UK) was added for 1 hour, followed by substrate washing as described above. FITC-conjugated streptavidin was added (1:50 in 1% BSA/PBS, Vector Laboratories UK) for 2 hours before samples were given a final wash. Samples were mounted using mounting medium for fluorescence, with DAPI counterstain (Vector Laboratories), and viewed by fluorescent microscopy (Zeiss Axiophot).

In-cell Western

Cells were fixed and permeabilised as per immunocytochemistry. Afterwards, non-specific binding sites were blocked with PBS/1% milk protein for 1.5 hours at room temperature with gentle agitation on a plate shaker. Samples were incubated in PBS/1% milk protein containing anti-KLF2 antibody H60 (sc-28675, Santa Cruz Biotechnology, CA, USA) primary antibody (1:50) and GAPDH primary antibody (1:10000, mouse monoclonal antihuman, Sigma Aldrich, UK) for 2 hours at 37°C. Samples were washed five times in 0.1% PBS/Tween 20 with gentle agitation (5 minutes each). Samples were then incubated for 1 hour with gentle agitation in secondary antibodies (donkey anti mouse IR680RD and donkey anti rabbit IR800CW, 1:500, Li-cor UK) diluted in PBS/1% milk protein containing 0.2% Tween 20. The samples were then washed five times in 0.1% PBS/Tween, as previously described. Wells were dried and analysed using the Licor Odyssey Imaging System. Readings at 700 nm and 800 nm were taken and quantified in excel.

RESULTS AND DISCUSSION

Thermoresponsive ink properties and fabrication of polymer arrays

The thermoresponsive nature of polymers can arise from various structural properties such as the presence of a thermosensitive polymer backbone[45,46] or by thermosensitive units linked on the polymer chains.[47,48] Among these systems exhibiting thermoresponsive behaviour, N-substituted poly(acrylamides) are one of the most extensively investigated polymers, especially due to their known biocompatibility.[49] In addition, N-alkyl acrylamides can be copolymerised with other stimuli-responsive monomers to combine characteristics of different monomeric units

in a single system. Recently, a range of commercially available amino-terminated copolymers of ethylene oxide and propylene oxide, known as Jeffamines, have also been shown to possess thermoresponsive properties.[50,51]

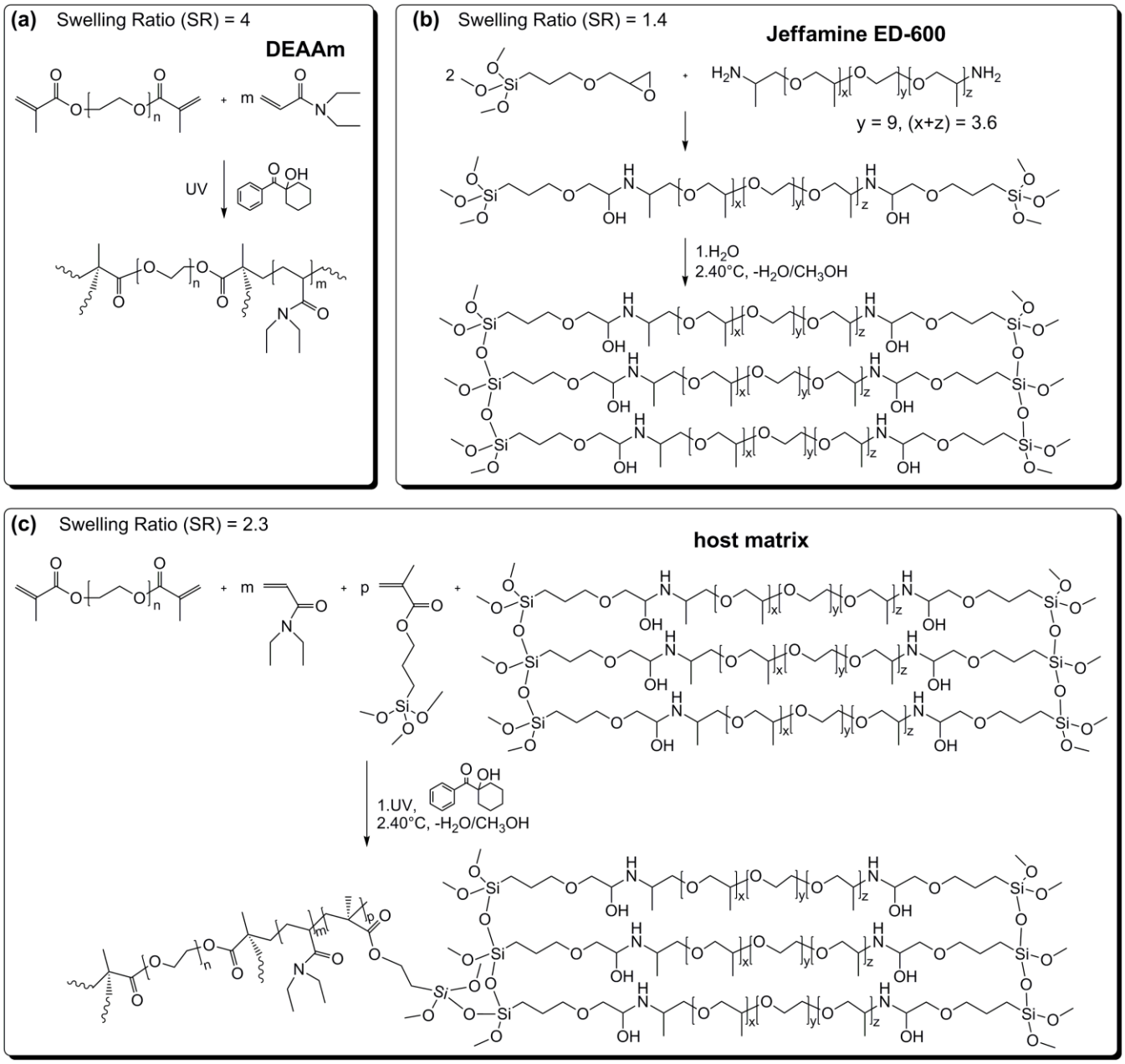

Figure 1. (a) Chemical reaction for the ink with N,N-diethylacrylamide (DEAAm) as thermoresponsive component, (b) Jeffamine ED-600 and (c) for the mixed system using DEAAm and the Jeffamine-based gel as host matrix.

The development of a suitable thermoresponsive ink for DPN printing was one of the most crucial phases in our work. We investigated different thermoresponsive inks and compared their ink transport and writing capabilities. We first studied a UV-curable ink mainly composed of N,N-diethylacrylamide (DEAAm) acting as a thermoresponsive monomer with a small percentage of crosslinker and photoinitiator (Figure 1 (a)). To covalently bond the thermoresponsive structures patterned by DPN to silicon oxide substrates, two different silanes, one with a methacrylate end functional group and another one with a terminal thiol, were investigated for the functionalisation of the silicon surface. The transfer of this thermoresponsive ink from the inked tip onto the two substrates, however, was dominated by the volatility of DEAAm in air. Due to its high volatility, DEAAm becomes even more volatile at the microscale. UV-cured micron–sized spots deposited by DPN showed a Raman spectrum very similar to that of the crosslinker, because the monomer in the ink had evaporated during the loading of the tip and the printing process (*See supporting information, Figure S1*). The printing experiments were performed at room temperature (22-23°C) and at a rather low percentage of relative humidity (25-35%). An increase of the temperature did not improve ink transport and patterning because it caused an increased vaporisation of DEAAm. In addition, a higher relative humidity accelerates the process of evaporation of DEAAm due to the high solubility of DEAAm in water, which causes liquid DEAAm to convert into a gas more rapidly. To solve this issue, we examined an ink with Jeffamine ED-600 (Figure 1 (b)). Due to the presence of Jeffamine, the ink exhibited a hydrophilicity higher than the UV-curable material which resulted in it spreading across surfaces such as bare and methacrylate-silanised silicon oxide. Reproducible polymer arrays were created only on thiol-silanised silicon oxide substrates (Figure 2(a)), which turned out to be hydrophobic enough to prevent the spreading of the Jeffamine ink.

Figure 2 (a) shows a white light image of the printed arrays with Jeffamine ink and (c) displays an AFM topography image of a small area within the same region. Figure 2 (e) shows the height profile measured across two array spots. The increased viscosity of the Jeffamine ED-600 (75 cp) allowed for improvement of the kinetics of ink flow from the tip to the substrate and enabled the printing of large sets of arrays, without the need to re-ink the tip. The bulk material of Jeffamine ink after heat-curing showed a swelling ratio of 1.4 which is lower than that of the UV-cured DEAAm bulk sample (≈ 4). Moreover, a reversible switch was not observed across the transition temperature for the Jeffamine bulk samples.

To create patterns with a higher degree of swelling and a reversible temperature-induced switch, the combination of these two systems was also studied. The ink composed of Jeffamine can be used not only as a thermoresponsive component but also as a carrier matrix. The addition of the Jeffamine matrix having hydroxyl and secondary amine groups capable of polar interactions and hydrogen bonding with the amide group of DEAAm, can reduce the evaporation of DEAAm and improve the ink transport. After preparing the Jeffamine ink, we added the DEAAm ink prepared as mentioned previously, as well as a silane with a methacrylate terminal group to covalently link the Jeffamine matrix to the acrylamide network (Figure 1 (c)). This mixed system (from here on referred to as Jeffamine/DEAAm) exhibited a swelling ratio of 2.3, an intermediate value between those measured for the other inks investigated. The increased swelling ratio of the mixed system in comparison to the Jeffamine alone is due to the larger swelling weight of the Jeffamine/DEAAm at room temperature, which can be attributed to the less packed hydrogel structure of this system and the fact that the water-polymer interactions in the Jeffamine/DEAAm are more thermodynamically favoured at 20°C than when the Jeffamine is present alone. Less difference in swelling weight is observed at 40°C due to the less packed

polymerized structure which favours hydrophobic interactions in the polyDEAAm chains, causing the Jeffamine/DEAAm to de-swell in the same way that the Jeffamine does. Similarly to the Jeffamine ink system, large sets of arrays with consistently sized features were also obtained when printing with the Jeffamine/DEAAm ink (Figure 2 (b) and (d)).

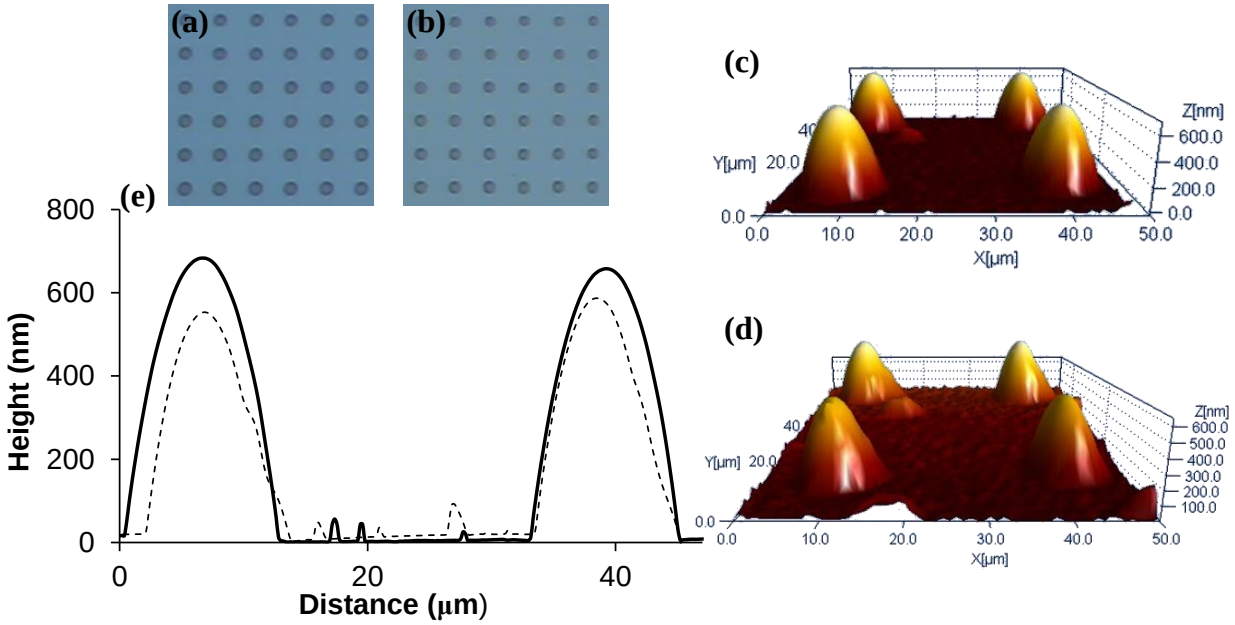

Figure 2. Optical images of (a) Jeffamine and (b) Jeffamine/DEAAm arrays printed by DPN using a 0.5 s dwell time. (c) and (d) AFM topography images from selected areas of the arrays shown in (a) and (b), respectively. (e) Height profiles of two array spots from the images shown in (c) (solid line) and (d) (dashed line) from the Jeffamine and Jeffamine/DEAAm arrays, respectively.

As part of the optimisation process and to determine whether spot size could be controlled, the dwell time (length of time the tip is in contact with the surface during printing) was varied and AFM images were collected of the resulting arrays. Arrays were patterned using the M-type pen arrays with 12 individual pens and three random spots from three different sets of arrays were

analysed using AFM. Figure 3 shows the plot of dwell time against (a) spot height and (b) spot diameter for both the Jeffamine and Jeffamine/DEAAm inks. It can be observed here that there is a general increase in both spot height and diameter with increasing dwell time for each of the two inks. The height of the spots patterned in this study with Jeffamine ink ranged from about 605 nm up to 720 nm by varying the dwell time from 0.1 s to 1 s. The smallest spot diameter obtained was 11 μm using a 0.1 s dwell time which increased up to nearly 15 μm using a dwell time of 1 s. For the Jeffamine/DEAAm ink, the printed spots were smaller, ranging from 546 nm to 654 nm in height and from about 9 μm to around 13 μm in diameter. The observed difference in spot size could be attributed to a slight change in viscosity between the two inks or the fact that the arrays were printed using different tips. It is important to note that the size of spots can vary between different surfaces and tips and therefore a standard size range should be tested to determine a relationship between dwell time and spot size in individual cases. However, the general increase with increasing dwell time for both ink systems indicates that feature size can be controlled by the straightforward adjustment of printing conditions.

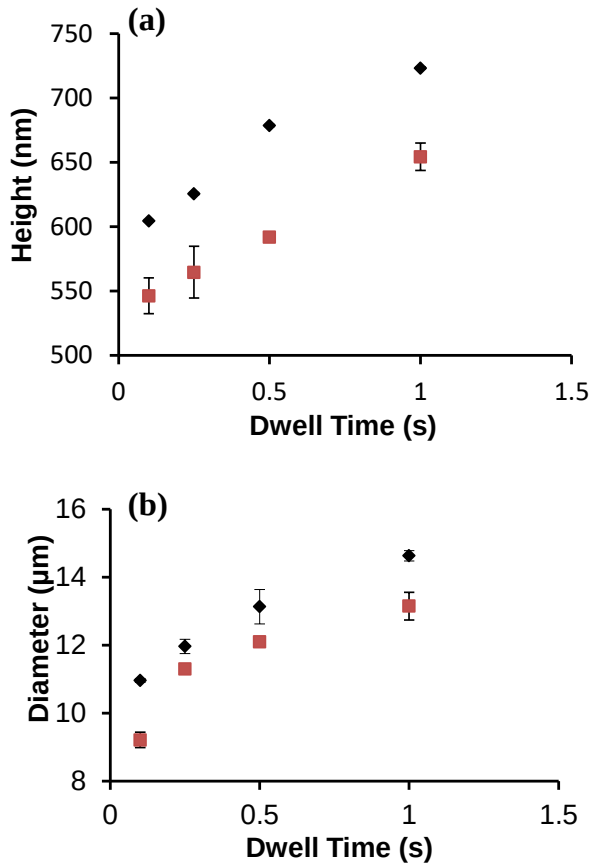

Figure 3. Plot of dwell time against spot height (a) and spot diameter (b) for the Jeffamine ED-600 arrays (black) and the Jeffamine/DEAAm arrays (red).

Chemical Characterisation of Printed Arrays

Raman spectroscopy was used to characterise the array spots after printing and curing and the resulting spectra were compared to those of the bulk material. Figure 4 (a) shows that the spectrum of the Jeffamine array spot has the same peaks as those obtained from the bulk material. There is also a good agreement between the peak vibration frequencies obtained for Jeffamine bulk material and the spot deposited by DPN in the 1200 - 3500 cm^{-1} region (Table S1) and thus it can be confirmed that the array spots contain the same components as the original ink.

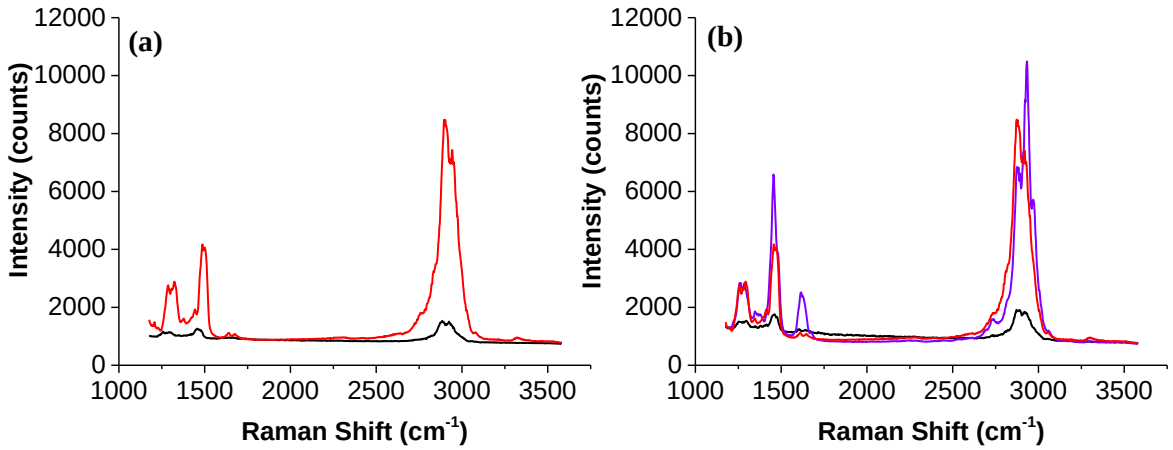

Figure 4. (a) Raman spectra of the Jeffamine bulk material (red) and array spot (black) (b) Raman spectra of the Jeffamine/DEAAm bulk material (blue), corresponding array spot (black) and Jeffamine bulk material (red). Spectra were obtained using a 633 nm laser excitation wavelength and 5 x 10 s accumulations.

Figure 4 (b) compares the Raman spectra of the Jeffamine/DEAAm ink (bulk and printed spot) and the Jeffamine bulk material. The spectrum of Jeffamine/DEAAm bulk material has a relatively strong band in the C=C and C=O stretch region (the peak of C=C stretching at 1615 cm^{-1} and a shoulder of tertiary amide C=O stretching at 1673 cm^{-1}). The absence of such similar bands in the C=C and C=O stretch region in the spectrum obtained from the Jeffamine/DEAAm spot led to the suggestion that spots printed with the mixed ink system were only composed of Jeffamine. However, differences between Jeffamine and Jeffamine/DEAAm array spots were observed in the thermoresponsive properties and these are shown in the following section. Consequently, this suggests the presence of polyacrylamide chains in the array spots created with the mixed system, even though their composition seems rather different from the original ink.

Thermoresponsive properties of patterns

In order to assess the thermoresponsive behaviour of the polymer arrays, we investigated the changes in the array spots which occurred in aqueous solution and when heated across the LCST. Raman scattering was first used to investigate any structural changes taking place as a result of the interactions between the polymer and water molecules. Previous studies have shown that changes in Raman spectra of thermoresponsive polymers can be observed across the LCST.[52,53] Arrays printed using a 0.5 s dwell time were analysed dry before being left in water for 72 h to allow equilibrium swelling to be reached. After collecting the Raman spectra of the arrays in water, the temperature was increased to 37 °C and the arrays were again left for 72 h to allow the system to equilibrate. Resulting spectra can be found in Figure 5 (a) and (b) for the Jeffamine and Jeffamine/DEAAm, respectively. This shows that, as well as the appearance of the OH stretch between 3000 cm^{-1} and 3500 cm^{-1} and the OH bending mode at around 1600 cm^{-1}, there is a change in the ratio of the symmetric and asymmetric CH stretches when the arrays are in water. The observed OH stretch is broad and flat which can be attributed to the interaction of the water molecules with the polymer and thus the restriction in position and orientation of the water molecules. There is also a shift in frequency in the OH bending mode upon heating, as well as an increase in intensity and narrowing of the band, which is typically found due to the weakening of hydrogen bonds and the strengthened OH bonds.[54] The area under the peaks was calculated so that the ratios could be compared more accurately, and it was found that the ratio of the symmetric CH stretch : asymmetric CH stretch decreased between the dry arrays and arrays in water and upon heating, increased to an intermediate point (Table 1). This indicates that the decrease is coinciding with increasing water content and thus confirms the temperature-induced

changes in the polymer array spots. It is also shown here that the ratio of the OH stretch : CH stretch changes significantly before and after heating and the decrease in this ratio is consistent with water being expelled on collapsing/de-swelling of the polymer microspot. Furthermore, the changes which can be observed in the ratio of the OH stretch : CH stretch before and after heating are more significant in the Jeffamine/DEAAm than in the Jeffamine alone, indicating that the thermoresponsive properties are greater in this system. Additionally, the differences in the Raman spectra are consistent with the changes in swelling ratio which are observed between the two systems in bulk. The increased water content of the Jeffamine/DEAAm system at room temperature is apparent in the Raman spectra where the ratio of the OH stretch : CH stretch is greater for the Jeffamine/DEAAm array spot in water at room temperature. Therefore, even although the microspot spectrum is different from that of the bulk material (Figure 4 (b)), the polyacrylamide chains are present in the microspot resulting in an increase in the swelling properties when compared to those of the Jeffamine alone. AFM was then used to analyse the array spots before and after heating in order to determine whether changes in topography could be observed. After leaving the arrays in water for 72 h to allow equilibrium swelling to be reached, AFM images were collected. The arrays were then left for a further 72 h at 37°C and AFM images were collected in the same way. In order to ensure a fair comparison, registration marks on the silicon dioxide surface were used to allow the exact same areas to be scanned before and after heating so that the height and diameter of the same spots, before and after heating, could be compared. Figure 5 (c) and (d) show the AFM data of the Jeffamine spots and the Jeffamine/DEAAm, respectively. In the Jeffamine/DEAAm in particular, when the height profiles before and after heating are compared, we can see a clear decrease in height and increase in diameter which indicates that the polymer is de-swelling or collapsing upon heating. The fact

that this change is less clear for the Jeffamine alone further confirms that the introduction of DEAAm into this system has led to an improvement in the thermoresponsive properties. This data can be seen more clearly in Table 2 where the actual changes in height and diameter are noted. The average sizes in this table were taken from the AFM images of three different spots before and after heating. The changes in height and diameter which have been observed show that, by increasing the temperature above the transition point, we can achieve a change in topography of the polymer microstructures on the surface. This temperature-induced change in topography creates a controllable surface which could be useful in a variety of applications such as cell culture, drug delivery and tissue regeneration.

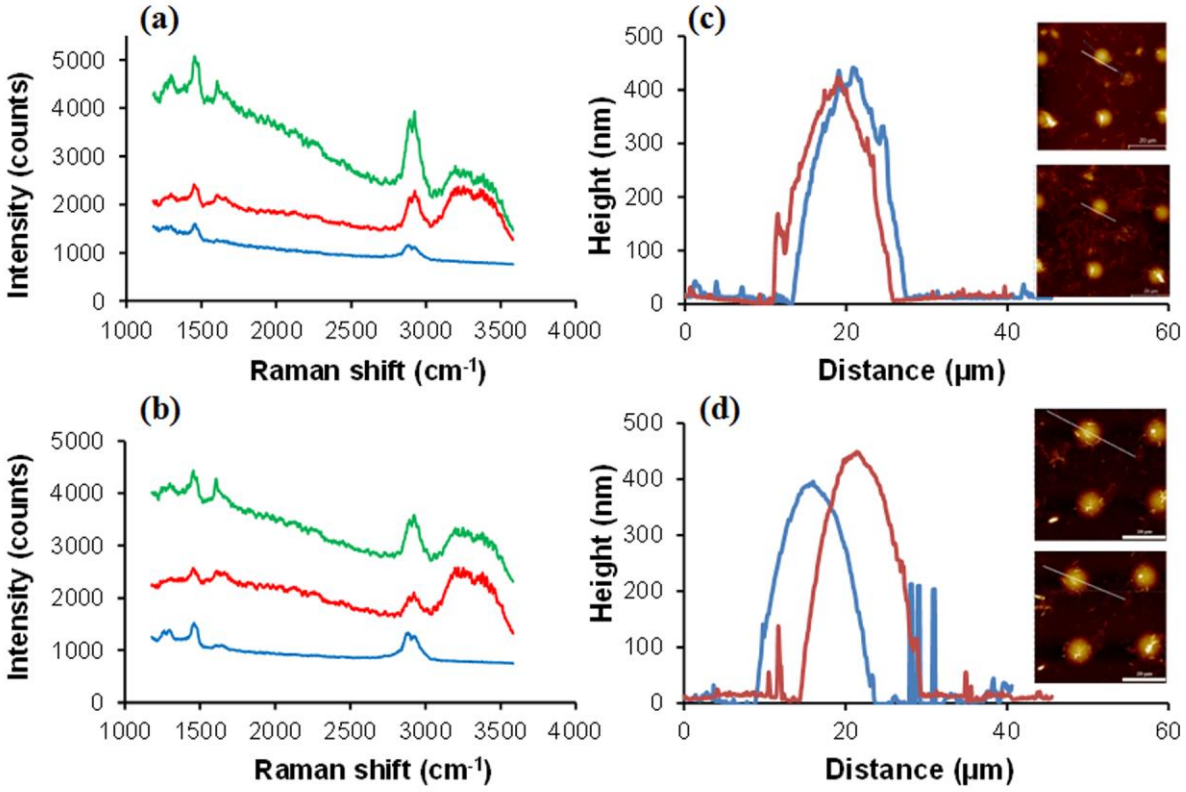

Figure 5. (a) Raman spectrum of dry Jeffamine array spot in air (blue), array spot immersed in water at room temperature (red) and array spot in water with heating (green). (b) Corresponding Raman spectra from arrays of Jeffamine/DEAAm. Spectra were collected using 633 nm laser

excitation with 5 x 10 second accumulations. (c) Height profile of Jeffamine array spot before (red) and after (blue) heating to 37°C. Inset: AFM images from which the height profiles were obtained with white lines highlighting the exact location of the corresponding profile. (d) Corresponding AFM data for Jeffamine/DEAAm array spots.

Table 1. Area under peaks corresponding to CH and OH stretching modes and comparison of peak ratios between dry arrays, arrays in water at room temperature and arrays in water at 37°C.

	Peak Ratio (CH Stretch (2835 – 2900 cm^{-1}):CH Stretch (2907 – 2963 cm^{-1}))	**Peak Ratio (OH Stretch (3046 cm^{-1} – 3552 cm^{-1}):CH Stretch (2835 cm^{-1} – 2963 cm^{-1}))**
Dry Arrays	Jeffamine: 2.08 ± 0.26 Jeffamine/DEAAm: 2.28 ± 0.09	-
Before Heating	Jeffamine: 0.51 ± 0.12 Jeffamine/DEAAm: 0.74 ± 0.14	Jeffamine: 7.38 ± 0.17 Jeffamine/DEAAm: 16.24 ± 1.90
After Heating	Jeffamine: 0.84 ± 0.06 Jeffamine/DEAAm: 0.85 ± 0.08	Jeffamine: 2.74 ± 0.48 Jeffamine/DEAAm: 5.29 ± 0.33

Table 2. Changes in height and diameter of Jeffamine and Jeffamine/DEAAm array spots in water after heating to 37°C.

	Average Height Change (nm)	**Average Diameter Change (μm)**
Jeffamine	- 33.0 ± 6.1	+ 0.2 ± 0.11
Jeffamine/DEAAm	- 68.0 ± 12.6	+ 0.6 ± 0.05

Cellular response to thermoresponsive polymer arrays

In order to observe potential cell responses, we cultured endothelial cells, which have previously been shown to respond to small changes in surface topography,[55] on the patterned surfaces in both swollen and de-swollen states. The LE2 cells were cultured on surfaces printed with Jeffamine/DEAAm arrays using a 1 s dwell time with features spaced 22 µm apart. At first this was performed only at 37ºC, standard culture conditions, for 4 days and vinculin staining of cell adhesions showed regular interaction with the posts (Figure 6 (a)). The interaction tended to result in adhesions forming around, rather than on, the posts. This became clearer with actin cytoskeleton staining and vinculin staining showing adhesions around the posts and membrane invaginations occurring where the cells contacted the posts (Figure 6 (b)). After ascertaining that the endothelial cells adhered, spread and interacted with the features, we next looked at phenotype through in-cell western analysis in Krüppel-like Factor 2 (KLF2), an endothelial transcription factor with roles in angiogenesis.[56] Analysis indicated that while KLF2 expression reduced in cells on the patterned surfaces compared to planar controls at 37ºC suggesting loss of phenotype with post interaction, at 33ºC this loss of expression in response to posts was not seen and KLF2 levels remained the same as on controls at 33ºC and 37ºC (Figure 6 (c)). Further analysis allows us to postulate that this may be due to altered cellular interaction with posts at the lower temperature resulting in maintained KLF2 expression (Figure 6 (d)). While the mean values for number of interactions are similar at 4.8±2.8 for 37ºC and 4.9±2.7 for 33ºC, the adhesion spread is different. At 33ºC, there is less data spread with many cells having 4-6 feature interactions. However, at 37ºC, the data is spread out with a notable increase in cells with many interactions in the 10-12 range. Although these results are preliminary, it is interesting to note

that the cells are interacting well with the polymer features and that a difference in the cell behaviour can be observed across the transition temperature, indicating the potential use of the surfaces in biological applications.

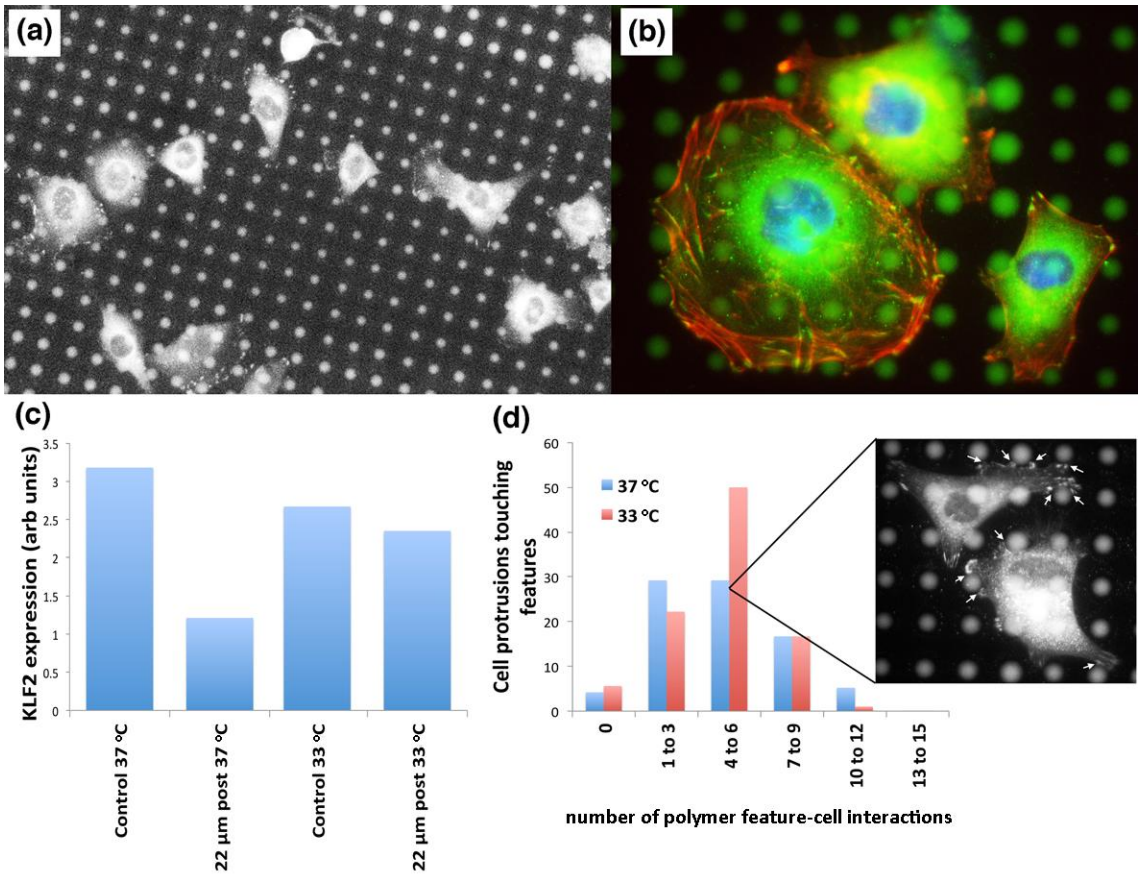

Figure 6. (a) Vinculin staining (adhesions seen as white lines within the cell boundaries) showing that adhesions form around rather than on the printed features (arrows point to adhesions close to posts). (b) Actin (red) and vinculin (green) staining showing that this adhesion pattern causes membrane invaginations to form around the posts (arrows point to invaginations around posts) (nuclei are blue). (c) KLF2 expression showing that the features prevent loss of KLF2 expression with reduced temperature (n=1). (d) Quantification of number of features individual cells interact with, showing that cells interact more strongly with the posts at lower

temperature (arrows show vinculin positive adhesions close to features) (50 cells counted per substrate).

CONCLUSIONS

Dip-pen nanolithography has been used for the consistent patterning of thermoresponsive polymer arrays onto a thiol-silanised silicon dioxide substrate with significant control over feature size. A novel ink formulation based on Jeffamine ED-600 has been developed and we have shown that this can act as a carrier matrix to improve the printing of DEAAm whilst also increasing the swelling properties of the hydrogel when compared to the Jeffamine ink alone. Characterisation of the arrays by Raman and AFM has shown that, as well as a change in hydration state of the polymer, a temperature-induced change in topography of the arrays on the surface can be observed. We envisage that this thermally controlled switchable surface could be useful in a variety of applications ranging from cell culture to micro-actuators for microfluidic devices. Preliminary experiments show that cells adhere to and interact with the polymer features and that a change in cell behaviour is observed with changing temperature. This indicates that the controllable surfaces are biocompatible and have potential use for cellular applications.

ASSOCIATED CONTENT

Supporting Information. Figure S1. Comparison of Raman spectra of the DEAAm printed spot, the PEG-DMA crosslinker and the whole ink solution. Table S1. Table of Raman vibration assignments for the printed array spots and bolk material of Jeffamine and Jeff/DEAAm ink systems. This material is available free of charge via the Internet at http://pubs.acs.org.

AUTHOR INFORMATION

Corresponding Author

*Prof. Duncan Graham, Centre of Molecular Nanometrology, Technology and Innovation Centre, University of Strathclyde, 99 George Street, Glasgow G1 1RD, United Kingdom.

duncan.graham@strath.ac.uk

Author Contributions

The manuscript was written through contributions of all authors. All authors have given approval to the final version of the manuscript. #These authors contributed equally.

Funding Sources

Stacey Laing, Karen Faulds and Duncan Graham received funding from The Leverhulme Trust (Research Project Grant RPG-2012-758) and EPSRC Doctoral Training Programme awards (EP/P503574/1, EP/P505127/1 and EP/P504325/1). Raffaella Suriano obtained support from Progetto Bandiera "La Fabbrica del Futuro" in the framework of the funded project "POLYPHAB, POLYmer nanostructuring by two-PHoton ABsorption. M.J.D. and D.G. were awarded funding from BBSRC (grant no. BB/K006908/1).

Notes

The research data associated with this paper will become available at the following link:

http:// 10.15129/b442c62a-8ff2-4854-972e-8d861e9b2aed

ACKNOWLEDGMENT

The authors acknowledge Dr. Laura McNamara for her help in carrying out the cell experiments. K.F. and S.L. thank the Leverhulme Trust through Research Project Grant RPG-2012-758 for funding. D.G. acknowledges the Analytical Chemistry Trust Fund, EPSRC for the award of an analytical studentship which supported and funded this work. R.S. would also like to acknowledge support by Progetto Bandiera "La Fabbrica del Futuro" in the framework of the funded project "POLYPHAB, POLYmer nanostructuring by two-PHoton ABsorption. M.J.D and D.G. thank BBSRC for funding through award no. BB/K006908/1.

REFERENCES

1. Seliktar, D., Designing Cell-Compatible Hydrogels for Biomedical Applications. *Science* **2012,** *336* (6085), 1124-1128.

2. Kopecek, J., Hydrogel Biomaterials: A Smart Future? *Biomaterials* **2007,** *28* (34), 5185-5192.

3. Tanaka, T.; Fillmore, D.; Sun, S. T.; Nishio, I.; Swislow, G.; Shah, A., Phase Transitions in Ionic Gels. *Phys. Rev. Lett.* **1980,** *45* (20), 1636-1639.

4. Tanaka, T., Collapse of Gels and Critical Endpoint. *Phys. Rev. Lett.* **1978,** *40* (12), 820-823.

5. Vancoillie, G.; Frank, D.; Hoogenboom, R., Thermoresponsive Poly(Oligo Ethylene Glycol Acrylates). *Prog. Polym. Sci.* **2014,** *39* (6), 1074-1095.

6. Suzuki, A.; Tanaka, T., Phase Transition in Polymer Gels Induced by Visible Light. *Nature* **1990,** *346* (6282), 345-347.

7. Lee, H. I.; Wu, W.; Oh, J. K.; Mueller, L.; Sherwood, G.; Peteanu, L.; Kowalewski, T.; Matyjaszewski, K., Light-induced Reversible Formation of Polymeric Micelles. *Angew. Chem. Int. Ed.* **2007,** *46* (14), 2453-2457.

8. Tanaka, T.; Nishio, I.; Sun, S. T.; Uenonishio, S., Collapse of Gels in an Electric Field. *Science* **1982,** *218* (4571), 467-469.

9. Brun-Graeppi, A. K. A. S.; Richard, C.; Bessodes, M.; Scherman, D.; Merten, O.-W., Thermoresponsive Surfaces for Cell Culture and Enzyme-free Cell Detachment. *Prog. Polym. Sci.* **2010,** *35* (11), 1311-1324.

10. Rodriguez-Hernandez, J.; Checot, F.; Gnanou, Y.; Lecommandoux, S., Toward 'Smart' Nano-objects by Self-assembly of Block Copolymers in Solution. *Prog. Polym. Sci.* **2005,** *30* (7), 691-724.

11. Roy, D.; Brooks, W. L. A.; Sumerlin, B. S., New Directions in Thermoresponsive Polymers. *Chem. Soc. Rev.* **2013,** *42* (17), 7214-7243.

12. Zhang, Q.; Hoogenboom, R., Polymers with Upper Critical Solution Temperature Behavior in Alcohol/Water Solvent Mixtures. *Prog. Polym. Sci.* **2015,** *48*, 122-142.

13. Schmaljohann, D., Thermo- and pH-Responsive Polymers in Drug Delivery. *Adv. Drug Delivery Rev.* **2006,** *58* (15), 1655-1670.

14. Klouda, L.; Mikos, A. G., Thermoresponsive Hydrogels in Biomedical Applications. *Eur. J. Pharm. Biopharm.* **2008,** *68* (1), 34-45.

15. Otake, K.; Inomata, H.; Konno, M.; Saito, S., Thermal Analysis of the Volume Phase-transition with N-isopropylacrylamide Gels. *Macromolecules* **1990,** *23* (1), 283-289.

16. Lin, S. Y.; Chen, K. S.; Liang, R. C., Thermal Micro ATR/FT-IR Spectroscopic System for Quantitative Study of the Molecular Structure of poly(N-isopropylacrylamide) in Water. *Polymer* **1999,** *40* (10), 2619-2624.

17. Flory, P. J., *Principles of Polymer Chemistry*. First ed.; Cornell University Press: Ithaca, United States, 1953.

18. Okano, T.; Yamada, N.; Okuhara, M.; Sakai, H.; Sakurai, Y., Mechanism of Cell Detachment from Temperature-modulated, Hydrophilic-hydrophobic Polymer Surfaces *Biomaterials* **1995,** *16* (4), 297-303.

19. Kushida, A.; Yamato, M.; Konno, C.; Kikuchi, A.; Sakurai, Y.; Okano, T., Decrease in Culture Temperature Releases Monolayer Endothelial Cell Sheets Together with Deposited Fibronectin Matrix from Temperature-responsive Culture Surfaces. *J. Biomed. Mater. Res.* **1999,** *45* (4), 355-362.

20. Nagase, K.; Kobayashi, J.; Kikuchi, A.; Akiyama, Y.; Kanazawa, H.; Okano, T., Interfacial Property Modulation of Thermoresponsive Polymer Brush Surfaces and Their Interaction with Biomolecules. *Langmuir* **2007,** *23* (18), 9409-9415.

21. Canavan, H. E.; Cheng, X. H.; Graham, D. J.; Ratner, B. D.; Castner, D. G., Surface Characterization of the Extracellular Matrix Remaining After Cell Detachment from a Thermoresponsive Polymer. *Langmuir* **2005,** *21* (5), 1949-1955.

22. Zhang, R.; Mjoseng, H. K.; Hoeve, M. A.; Bauer, N. G.; Pells, S.; Besseling, R.; Velugotla, S.; Tourniaire, G.; Kishen, R. E. B.; Tsenkina, Y.; Armit, C.; Duffy, C. R. E.; Helfen, M.; Edenhofer, F.; de Sousa, P. A.; Bradley, M., A Thermoresponsive and Chemically Defined Hydrogel for Long-term Culture of Human Embryonic Stem Cells. *Nat. Commun.* **2013,** *4*, 1335-1335.

23. Kavanagh, C. A.; Rochev, Y. A.; Gallagher, W. A.; Dawson, K. A.; Keenan, A. K., Local Drug Delivery in Restenosis Injury: Thermoresponsive Co-polymers as Potential Drug Delivery Systems. *Pharmacol. Ther.* **2004,** *102* (1), 1-15.

24. Ma, D.; Chen, H.; Shi, D.; Li, Z.; Wang, J., Preparation and Characterization of Thermo-responsive PDMS Surfaces Grafted with poly(N-isopropylacrylamide) by Benzophenone-initiated Photopolymerization. *J. Colloid Interface Sci.* **2009,** *332* (1), 85-90.

25. Okano, T.; Bae, Y. H.; Jacobs, H.; Kim, S. W., Thermally On Off Switching Polymers for Drug Permeation and Release. *J. Controlled Release* **1990,** *11* (1-3), 255-265.

26. Malmstadt, N.; Yager, P.; Hoffman, A. S.; Stayton, P. S., A Smart Microfluidic Affinity Chromatography Matrix Composed of poly(N-isopropylacrylamide)-coated Beads. *Anal. Chem.* **2003,** *75* (13), 2943-2949.

27. Luo, L.; Zhang, H.-S.; Liu, Y.; Ha, W.; Li, L.-H.; Gong, X.-L.; Li, B.-J.; Zhang, S., Preparation of Thermosensitive Polymer Magnetic Particles and Their Application in Protein Separations. *J. Colloid Interface Sci.* **2014,** *435*, 99-104.

28. Shekhar, S.; Mukherjee, M.; Sen, A. K., Synthesis and Characterization of Thermoresponsive Terpolymer for Protein Separation. *Int. J. Polym. Mater.* **2014,** *63* (8), 389-397.

29. Suzuki, H., Stimulus-responsive Gels: Promising Materials for the Construction of Micro Actuators and Sensors. *J. Intell. Mater. Syst. Struct.* **2006,** *17* (12), 1091-1097.

30. Kim, Y. S.; Liu, M.; Ishida, Y.; Ebina, Y.; Osada, M.; Sasaki, T.; Hikima, T.; Takata, M.; Aida, T., Thermoresponsive Actuation Enabled by Permittivity Switching in an Electrostatically Anisotropic Hydrogel. *Nat Mater* **2015,** *14* (10), 1002-1007.

31. Liu, F.; Jiang, S.; Ionov, L.; Agarwal, S., Thermophilic Films and Fibers from Photo Cross-linkable UCST-type Polymers. *Polym. Chem.* **2015,** *6* (14), 2769-2776.

32. Sershen, S. R.; Mensing, G. A.; Ng, M.; Halas, N. J.; Beebe, D. J.; West, J. L., Independent Optical Control of Microfluidic Valves Formed from Optomechanically Responsive Nanocomposite Hydrogels. *Adv. Mater.* **2005,** *17* (11), 1366-1368.

33. Ryu, S.; Yoo, I.; Song, S.; Yoon, B.; Kim, J.-M., A Thermoresponsive Fluorogenic Conjugated Polymer for a Temperature Sensor in Microfluidic Devices. *J. Am. Chem. Soc.* **2009,** *131* (11), 3800-3801.

34. Ahn, S. J.; Kaholek, M.; Lee, W. K.; LaMattina, B.; LaBean, T. H.; Zauscher, S., Surface-initiated Polymerization on Nanopatterns Fabricated by Electron-beam Lithography. *Adv. Mater.* **2004,** *16* (23-24), 2141-2145.

35. Jones, D. M.; Huck, W. T. S., Controlled Surface-initiated Polymerizations in Aqueous Media. *Adv. Mater.* **2001,** *13* (16), 1256-1259.

36. Kaholek, M.; Lee, W. K.; LaMattina, B.; Caster, K. C.; Zauscher, S., Fabrication of Stimulus-responsive Nanopatterned Polymer Brushes by Scanning-probe Lithography. *Nano Lett.* **2004,** *4* (2), 373-376.

37. Lee, W.-K.; Whitman, L. J.; Lee, J.; King, W. P.; Sheehan, P. E., The Nanopatterning of a Stimulus-responsive Polymer by Thermal Dip-pen Nanolithography. *Soft Matter* **2008,** *4* (9), 1844-1847.

38. Salaita, K.; Wang, Y.; Mirkin, C. A., Applications of Dip-pen Nanolithography. *Nat. Nanotechnol.* **2007,** *2* (3), 145-155.

39. Su, M.; Aslam, M.; Fu, L.; Wu, N. Q.; Dravid, V. P., Dip-pen Nanopatterning of Photosensitive Conducting Polymer Using a Monomer Ink. *Appl. Phys. Lett.* **2004,** *84* (21), 4200-4202.

40. Hernandez-Santana, A.; Irvine, E.; Faulds, K.; Graham, D., Rapid Prototyping of poly(dimethoxysiloxane) Dot Arrays by Dip-pen Nanolithography. *Chem. Sci.* **2011,** *2* (2), 211-215.

41. Stiles, P. L., Direct Deposition of Micro- and Nanoscale Hydrogels using Dip Pen Nanolithography (DPN). *Nat. Methods* **2010,** *7* (8), I-II.

42. Rakickas, T.; Ericsson, E. M.; Ruzele, Z.; Liedberg, B.; Valiokas, R., Functional Hydrogel Density Patterns Fabricated by Dip-Pen Nanolithography and Photografting. *Small* **2011,** *7* (15), 2153-2157.

43. Garoff, H.; Ansorge, W., Improvements of DNA Sequencing Gels. *Anal. Biochem.* **1981,** *115* (2), 450-457.

44. Kitamura, H.; Okita, K.; Fujikura, D.; Mori, K.; Iwanaga, T.; Saito, M., Induction of Src-suppressed C Kinase Substrate (SSeCKS) in Vascular Endothelial Cells by Bacterial Lipopolysaccharide. *J. Histochem. Cytochem.* **2002,** *50* (2), 245-255.

45. Feil, H.; Bae, Y. H.; Feijen, J.; Kim, S. W., Effect of Comonomer Hydrophilicity and Ionization on the Lower Critical Solution Temperature of N-isopropylacrylamide Copolymers. *Macromolecules* **1993,** *26* (10), 2496-2500.

46. Fettaka, M.; Issaadi, R.; Moulai-Mostefa, N.; Dez, I.; Le Cerf, D.; Picton, L., Thermo Sensitive Behavior of Cellulose Derivatives in Dilute Aqueous Solutions: From Macroscopic to Mesoscopic Scale. *J. Colloid Interface Sci.* **2011,** *357* (2), 372-378.

47. Deguchi, S.; Akiyoshi, K.; Sunamoto, J., Solution Property of Hydrophobized Pullulan Conjugated with poly(ethylene oxide)-poly(propylene oxide)-poly(ethylene oxide) Block-Copolymer - Formation of Nanoparticles and Their Thermosensitivity. *Macromol. Rapid Commun.* **1994,** *15* (9), 705-711.

48. Mocanu, G.; Mihai, D.; Dulong, V.; Picton, L.; Lecerf, D., New Anionic Amphiphilic Thermosensitive Pullulan Derivatives. *Carbohydr. Polym.* **2011,** *84* (1), 276-281.

49. Hatakeyama, H.; Kikuchi, A.; Yamato, M.; Okano, T., Bio-functionalized Thermoresponsive Interfaces Facilitating Cell Adhesion and Proliferation. *Biomaterials* **2006,** *27* (29), 5069-5078.

50. Agut, W.; Brulet, A.; Taton, D.; Lecommandoux, S., Thermoresponsive Micelles from Jeffamine-b-poly(L-glutamic acid) Double Hydrophilic Block Copolymers. *Langmuir* **2007,** *23* (23), 11526-11533.

51. Mocanu, G.; Mihai, D.; Dulong, V.; Picton, L.; Le Cerf, D., New Anionic Crosslinked Multi-responsive Pullulan Hydrogels. *Carbohydr. Polym.* **2012,** *87* (2), 1440-1446.

52. Schmidt, P.; Dybal, J.; Rodriguez-Cabello, J. C.; Reboto, V., Role of Water in Structural Changes of poly(AVGVP) and poly(GVGVP) Studied by FTIR and Raman Spectroscopy and ab initio Calculations. *Biomacromolecules* **2005,** *6* (2), 697-706.

53. Dybal, J.; Trchova, M.; Schmidt, P., The Role of Water in Structural Changes of poly(N-isopropylacrylamide) and poly(N-isopropylmethacrylamide) Studied by FTIR, Raman Spectroscopy and Quantum Chemical Calculations. *Vib. Spectrosc* **2009,** *51* (1), 44-51.

54. Praprotnik, M.; Janezic, D.; Mavri, J., Temperature Dependence of Water Vibrational Spectrum: A Molecular Dynamics Simulation Study. *J. Phys. Chem. A* **2004,** *108* (50), 11056-11062.

55. Dalby, M. J.; Riehle, M. O.; Johnstone, H.; Affrossman, S.; Curtis, A. S. G., In vitro Reaction of Endothelial Cells to Polymer Demixed Nanotopography. *Biomaterials* **2002,** *23* (14), 2945-2954.

56. Renz, M.; Otten, C.; Faurobert, E.; Rudolph, F.; Zhu, Y.; Boulday, G.; Duchene, J.; Mickoleit, M.; Dietrich, A.-C.; Ramspacher, C.; Steed, E.; Manet-Dupé, S.; Benz, A.; Hassel, D.; Vermot, J.; Huisken, J.; Tournier-Lasserve, E.; Felbor, U.; Sure, U.; Albiges-Rizo, C.; Abdelilah-Seyfried, S., Regulation of β1 integrin-Klf2-mediated Angiogenesis by CCM Proteins. *Dev. Cell* **2015,** *32* (2), 181-190.

For Table of Contents Only